Journal of Marine Science and Technology

Volume 23 | Issue 2 Article 9

EXPERIMENTAL STUDY OF SEISMIC PERFORMANCES OF RC BRIDGE COLUMNS WITH CFST COLUMN EMBEDDED LNSIDE

Wen-Liang Qiu
Department of Civil Engineering, Dalian University of Technology, Liaoning Province, China, P.R.C.

Chin-Sheng Kao
Department of Civil Engineering, Tamkang University, New Taipei City, Taiwan, R.O.C.

Chang-Huan Kou
Department of Civil Engineering, Chunghua University, Hsinchu City, Taiwan, R.O.C., chkou@chu.edu.tw

Jeng-Lin Tsai
Department of Civil Engineering, Chunghua University, Hsinchu City, Taiwan, R.O.C.

Recommended Citation

Qiu, Wen-Liang; Kao, Chin-Sheng; Kou, Chang-Huan; and Tsai, Jeng-Lin (2015) "EXPERIMENTAL STUDY OF SEISMIC PERFORMANCES OF RC BRIDGE COLUMNS WITH CFST COLUMN EMBEDDED LNSIDE," *Journal of Marine Science and Technology*: Vol. 23: Iss. 2, Article 9.
DOI: 10.6119/JMST-014-0612-1
Available at: https://jmstt.ntou.edu.tw/journal/vol23/iss2/9

EXPERIMENTAL STUDY OF SEISMIC PERFORMANCES OF RC BRIDGE COLUMNS WITH CFST COLUMN EMBEDDED LNSIDE

Acknowledgements

This study was funded by the National Natural Science Foundation of China (NSFC-51178080). The authors would like to acknowledge the Structure Engineering Laboratory of Dalian University of Technology for its support and constructive advice.

Journal of Marine Science and Technology, Vol. 23, No. 2, pp. 212-219 (2015)
DOI: 10.6119/JMST-014-0612-1

EXPERIMENTAL STUDY OF SEISMIC PERFORMANCES OF RC BRIDGE COLUMNS WITH CFST COLUMN EMBEDDED LNSIDE

Wen-Liang Qiu[1], Chin-Sheng Kao[2], Chang-Huan Kou[3], and Jeng-Lin Tsai[3]

Key words: composite columns, bridges, seismic effects, cyclic tests, damage, ductility.

ABSTRACT

To improve the seismic performances of reinforced concrete (RC) bridge columns and to prevent columns from shear failure and core concrete crushing, high strength concrete filled steel tube (CFST) is put into RC columns to form a new kind of composite column. Through cyclical loading tests, the seismic performances of four columns are studied. The first column tested is a conventional RC column, the second one is a bonded composite column, the third one is an unbonded composite column, and the fourth one is an unbonded composite column whose axial force is composed of only bone by its CFST column. The test results show that the CFST column can increase the flexural strength, displacement ductility and energy dissipation capacity, and decrease the residual displacement after undergoing large deformation. When the degree of bond between the steel tube and the outside concrete around the tube is reduced, the load-carrying capacity of the composite column decreases, but the ductility increases. When the axial force is only bone by the CFST column, the load-carrying capacity of the composite column decreases significantly, and the ductility increases markedly.

I. INTRODUCTION

Strong earthquakes occurring around the world have shown that the RC piers of girder bridges have two main failure modes, which lead to severe pier damages, such as collapse and other damages that make piers un-repairable (Chen and Duan, 1999; Hsu and Fu, 2004; Hashimoto et al., 2005). One mode is the shear failure resulting from the insufficient shear capacity of the column, and the other is core concrete crushing at the plastic hinge region due to the insufficient ductility of the column. Therefore, shear capacity and ductility are critically important to the seismic performances of bridge columns. To enhance the shear capacity and ductility of RC bridge columns, the generally used method is to increase the lateral reinforcements (Chen and Duan, 1999; Kao and Kou, 2010; Kao et al., 2010). Excessive use of reinforcements, however, can become counterproductive in terms of both constructability and economics (Pandey and Mutsuyoshi, 2005). It is thus important to find alternative methods of improving shear capacity and ductility to avoid relying heavily on lateral reinforcements alone.

Concrete filled steel tube (CFST) is a kind of composite structure which has many advantages, such as high flexural strength, compressive capacity and ductility (Roeder and Lehman, 2009). However, when used as a bridge column, CFST has many disadvantages. Because of the flexural capacity of CFST columns is high, the connection between CFST and the foundation is complicated and difficult (Roeder and Lehman, 2009). Additionally, the steel tube needs to be protected from corrosion.

In this paper, a CFST column is put into an RC pier to form a new kind of composite column. This kind of composite column takes advantage of both CFST and RC columns, and avoid their disadvantages. The composite column uses CFST to improve the shear capacity and ductility of the RC column, and avoids core concrete crushing at the plastic hinge region. Because the diameter of the CFST column in the composite column is small, only about 1/3 of the diameter of the RC column, it is easy to connect with the foundation.

To improve the ductility of the composite column, the concrete outside the steel tube is composed of normal strength concrete, which is more ductile than high strength concrete (Cusson and Paultre, 1994; Razvi and Saatcioglu, 1994). The concrete in the steel tube adopts high strength concrete to increase the compressive capacity of the CFST column. To further improve the ductility of the composite column, the degree of bond between the steel tube and the outside concrete

Paper submitted 06/29/12; revised 08/12/13; accepted 06/12/14. Author for correspondence: Chang-Huan Kou (e-mail: chkou@chu.edu.tw).
[1] *Department of Civil Engineering, Dalian University of Technology, Liaoning Province, China, P.R.C.*
[2] *Department of Civil Engineering, Tamkang University, New Taipei City, Taiwan, R.O.C.*
[3] *Department of Civil Engineering, Chunghua University, Hsinchu City, Taiwan, R.O.C.*

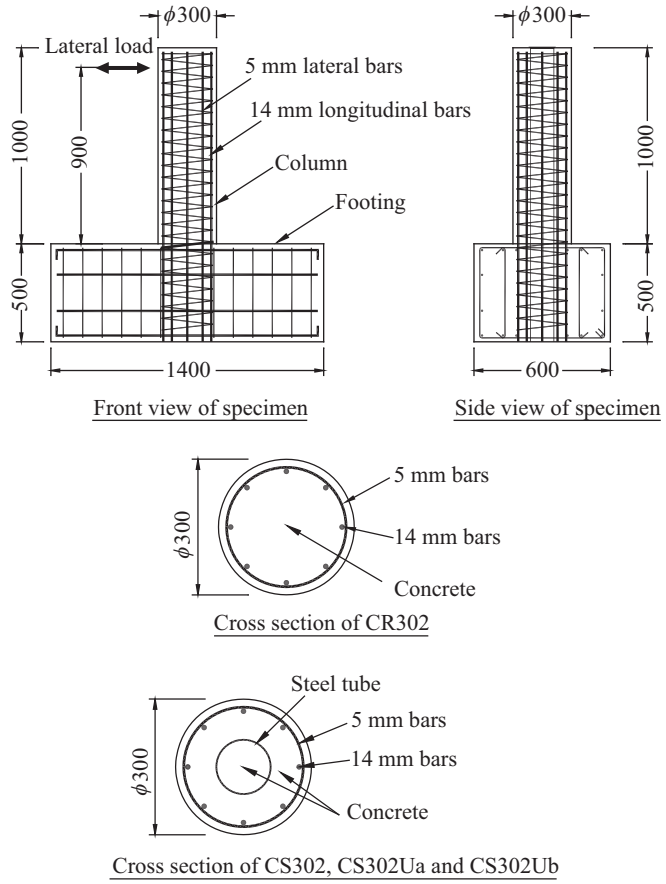

Fig. 1. Reinforcement details for specimens (units in mm).

around the tube is reduced to form an unbonded composite column.

To apply the kind of composite bridge column presented here in actual construction, seismic performances such as shear strength, flexural strength, ductility, residual displacement, and energy absorption capacity must be investigated. Therefore, four column specimens were tested to investigate the seismic performances of the composite column proposed in this study.

II. EXPERIMENTAL PROGRAM

1. Specimens

To investigate the seismic performances of the composite column with CFST embedded inside, four bridge column specimens with circular sections were designed in this study, as shown in Fig. 1. The diameter of each column was 300 mm and the height of the RC column was 1000 mm. The action point of the cyclic lateral load was at the height of 900 mm from the footing. Thus, the aspect ratio (the column height from the footing to the lateral load action point divided by the column diameter) was 3.0. The footing of the column was designed to be strong enough to avoid damage and reduce deformation of the footing. The footing was anchored to the strong floor by steel rods.

The alphanumeric designations of the four specimens were CR302, CS302, CS302Ua and CS302Ub. The column CR302 was a conventional RC column, which served as the comparative specimen with other columns. The other three columns were all composite columns with a CFST column embedded inside. For the columns CS302Ua and CS302Ub, two layers of plastic film were put between the steel tube and concrete outside of the tube to reduce the degree of bond and to make the slip between concrete and tube easier. Here, we call the columns CS302Ua and CS302Ub unbonded composite columns, and the column CS302 is called a bonded composite column. Therefore, the influences of the bond on seismic performances of composite columns could be investigated. The difference between CS302Ua and CS302Ub was that the height of the CFST column in CS302Ub was larger than the height of the RC column by 100 mm. The axial load of column CS302Ub acted on the top of CFST column. Thus, the RC column outside of the CFST column did not bear any axial load. The influences of axial load on seismic performances were investigated by experiments on columns CS302Ua and CS302Ub.

For column CS302Ub, its axial load index (ALI) was 0 because its RC column did not bear axial load. The ALI of the other three columns was designed to be about 0.2. The ALI is defined as the ratio of the axial load to the product of the specified compressive strength of concrete and the gross column cross section area.

2. Reinforcement, Concrete and Steel Tube

Each column was reinforced with eight longitudinal reinforcement bars evenly spaced in a circular pattern. The diameter of longitudinal reinforcement was 14 mm, and the reinforcement ratio was 1.74%. The lateral spiral reinforcement was a round bar with a diameter of 6 mm and a pitch of 50 mm. The clear concrete cover of lateral reinforcement was 25 mm in thickness. The yield stress of longitudinal reinforcement was 345 MPa, and the yield stress of lateral reinforcement was 235 MPa.

The concrete of column CR302 and the concrete outside the other three columns were composed of normal strength concrete with compressive strength of 32 MPa at 28 days. The concrete in the steel tube was high strength concrete with compressive strength of 54 MPa at 28 days. All of the concrete was constructed on the same day.

The diameter of the steel tubes in composite column specimens was 121 mm, and the thickness of the tube was 5.3 mm. The yield stress of the steel tube was 345 MPa. The length of the CFST column embedded in the footing was 450 mm.

3. Test Setup and Instrumentation

The seismic performance experiments on the specimens were accomplished in a structural testing laboratory with a servo-controlled hydraulic jack and a servo-controlled hydraulic actuator. Fig. 2 shows the test setup employed in this

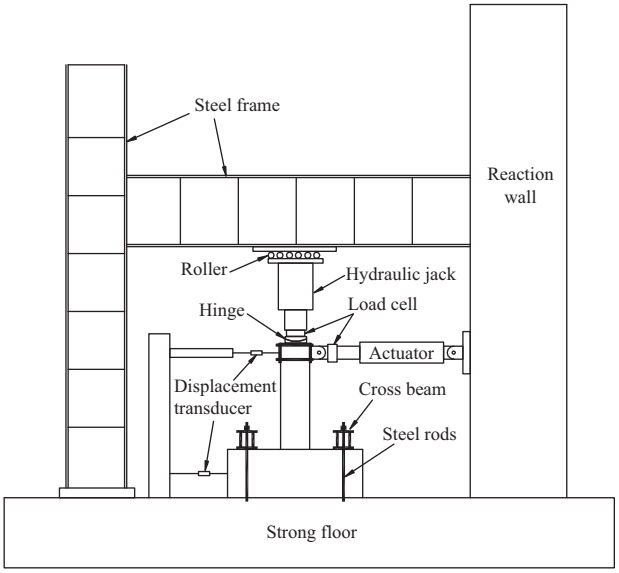

Fig. 2. Setup of experiment.

study. The axial load applied at the beginning of a test, which was kept constant during testing, was applied by a vertical hydraulic jack moved with the tip of a column. The cyclic lateral load was applied by a horizontal actuator. Two ends of the actuator were bolted to the reaction wall and the column head. The actuator had a capacity of 1000 kN and was capable of moving the column 150 mm in both pull and push direction. The vertical axial load was used to simulate the weight of the girder, and the cyclic lateral load was used to simulate the seismic load.

The load cells were used to measure and control the forces of the hydraulic jack and the actuator. Foil strain gauges on the surfaces of reinforcements and steel tube and displacement transducers at the top of the column and footing were used to record the responses of the column. Based on an ALI design of about 0.2, the axial loads applied on all specimens were 300 kN.

4. Experimental Procedure

The experimental procedure was established to ensure, to the extent possible, equal treatment of the four columns. 30 days after construction, the column specimen was moved into the laboratory and placed in the location shown in Fig. 2. After the specimen was plumbed, four rods were used to anchor the column footing to the floor. The axial load apparatus was then attached to the column. The instruments were placed on the column and attached to the data acquisition. The instruments were then calibrated. Finally, the horizontal actuator was attached to the column and then calibrated.

The data acquisition system was turn on and zeroed. The axial load was applied slowly using the servo-controlled hydraulic jack. The lateral load was applied using a servo-controlled hydraulic actuator at a quasi-static rate in displacement-controlled cycles with displacements of ±2 mm, ±4 mm,

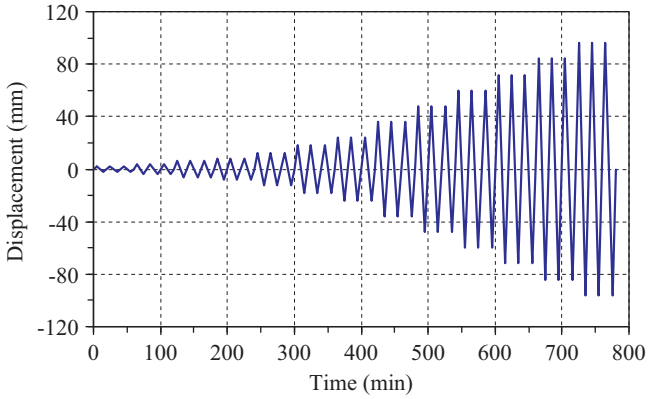

Fig. 3. Displacement history.

±6 mm, ±8 mm, ±12 mm, ±18 mm, ±24 mm, ±36 mm, ±48 mm, ±60 mm, ±72 mm, ±84 mm, ±96 mm, etc. The lateral displacement history is shown in Fig. 3. The column was cycled three times at each displacement level where a single displacement cycle consisted of pulling the actuator east and pushing the actuator west.

The instruments recorded the strains, displacements and loads throughout the entire course of testing. At the east peak and west peak of each displacement level, the widths of cracks were measured, dimensions of spalled regions were noted, the crack patterns on the east and west face were recorded, and photographs of observed damage and overall response were taken. Additional photographs were taken during testing at stages of important damage, such as buckling of longitudinal reinforcement, and fracturing of spiral reinforcement or longitudinal reinforcement.

When the core concrete of a column was crushed or the lateral load capacity of the column decreased to 80% of its maximum lateral load, testing was terminated.

III. EXPERIMANTAL RESULTS

1. Observed Responses

Fig. 4 gives the damage states of the four specimens at the end of the loading tests.

1) Column CR302

For CR302, when the top column lateral displacement amplitude reached 2 mm, there were no cracks occurring on the column, and the maximum lateral load in three cycles was 44.7 kN. When the lateral displacement amplitude reached 4 mm, several horizontal cracks occurred on each side of the column from the footing to the middle height of the column. The widths of the cracks were very small, and the cracks were closed under a zero lateral load in the actuator. The maximum lateral load in three loading cycles was 60.8 kN. In subsequent displacement amplitudes, the number of horizontal cracks only increased slightly, but the widths of the cracks increased markedly. When the lateral displacement amplitude reached

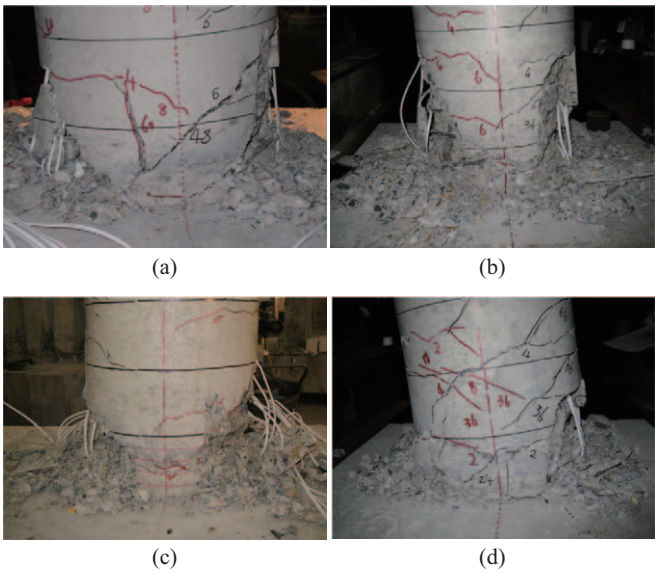

Fig. 4. Damage of specimens: (a) CR302; (b) CS302; (c) CS302Ua; and (d) CS302Ub.

18 mm, initial spalling of the cover concrete occurred near the footing. At the same time, several vertical cracks occurred. The maximum lateral load in three loading cycles was 85.5 kN. When the lateral displacement amplitude reached 24 mm, some blocks of cover concrete on both sides of the column in the loading direction spalled off. When the lateral displacement amplitude reached 36 mm, the spiral and longitudinal reinforcement on both sides of the column in the loading direction were exposed entirely because the cover concrete spalled off. The height of the spalling region was about 160 mm from the column footing. The maximum lateral load dropped to 82.7 kN, which is smaller than the previous maximum load. When the lateral displacement amplitude reached 48 mm, the spiral reinforcement extruded, and the longitudinal reinforcement buckled. At the same time, a diagonal shear crack occurred from the footing to the height of 190 mm. When the lateral displacement amplitude reached 60 mm, the spiral reinforcement yielded, the longitudinal reinforcement buckled seriously, and the lateral load capacity dropped to 57.5 kN. The loading test was terminated after the specimen underwent three cycles at the displacement amplitude of 72 mm because the lateral load capacity dropped to 34.6 kN.

2) Column CS302

When the lateral displacement amplitude was less than 48 mm, the cracking and cover concrete spalling of column CS302 were similar with those of column CR302. However, the maximum lateral load was 129.4 kN, which was larger than the maximum lateral load of column CR302 by 51.3%. The spalling height of the cover concrete from the footing was 140 mm, which was less than that of column CR302. No diagonal shear crack occurred in column CS302 during the loading test, which shows that the CFST column embedded in the RC column prevented shear failure. When the lateral displacement amplitude reached 60 mm, spiral reinforcement yielding and the longitudinal reinforcement buckling were not obvious observed. This shows that the CFST column in composite column shared a very significant part of the total axial load with the RC column, which postponed the buckling of longitudinal reinforcement. When the lateral displacement amplitude reached 72 mm, the longitudinal reinforcements began to buckle after three loading cycles. The lateral load capacity dropped to 88.4 kN, which was 80% smaller than the previous maximum lateral load, and the test was terminated.

3) Column CS302Ua

The observed responses of column CS302Ua were nearly the same as those of column CS302. The main difference between columns CS302Ua and CS302 was that the maximum lateral load of column CS302Ua was 115.2 kN, which is 89.0% of that of column CS302. The slip between concrete and steel tube reduced the lateral load capacity. When the lateral displacement amplitude reached 60 mm, longitudinal reinforcement buckling was not obvious. When the lateral displacement amplitude reached 72 mm, the longitudinal reinforcement began to buckle after three loading cycles. The loading test was terminated after one loading cycle at the displacement amplitude of 84 mm because a longitudinal reinforcement ruptured.

4) Column CS302Ub

The observed responses of column CS302Ub under cyclic lateral load were different from the other three columns at the beginning of loading. Horizontal cracks occurred when the lateral displacement amplitude was 2 mm. The number of cracks increased with increasing displacement amplitude, and the cracks were distributed evenly on the column body from the footing to the height of 700 mm. Because column CS302Ub had more cracks than the other columns, the widths of the crack were smaller. When the lateral displacement amplitude reached 36 mm, there was no cover concrete spalled off, but the crack at the height of 100 mm from footing was very wide. When the horizontal displacement amplitude reached 48 mm, some blocks of cover concrete on both sides of the column in the loading direction spalled off. Yielding of spiral bars and buckling of longitudinal reinforcement were not found during loading at the displacement amplitude of 72 mm. The spiral bars extruded and longitudinal reinforcements buckled at the displacement amplitude of 84 mm. Finally, the test ended because one of the longitudinal reinforcements ruptured during the first loading cycle at the displacement amplitude of 96 mm.

2. Load-Displacement Relationship

Fig. 5 shows the lateral load-displacement hysteretic curves of all of the columns subjected to the reversed cycling load. The lateral displacement of a column is the displacement at the point where the lateral load is applied. We found that the

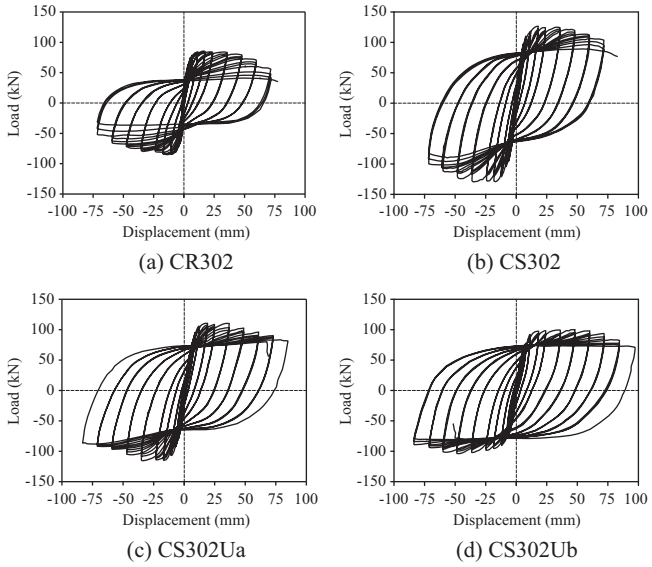

Fig. 5. Load-displacement hysteretic loops of specimens.

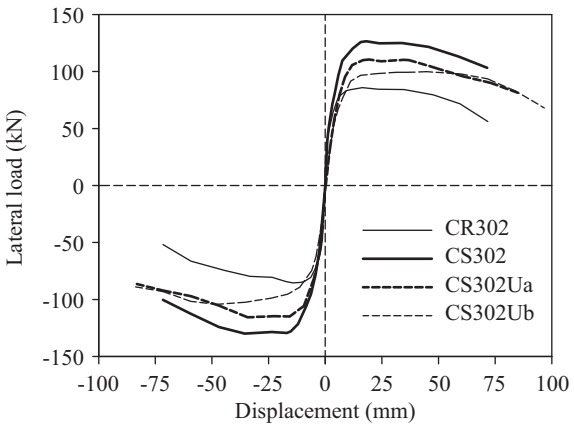

Fig. 6. Envelope curves of load-displacement hysteretic loop.

hysteretic curves of all the columns are very wide. All columns have ductile and stable behaviors under cyclic loads. For column CR302, the curves of three loading cycles at the same displacement amplitude are overlapped when the displacement amplitude is small. However, they separate from each other with increasing displacement amplitude. When the displacement amplitude is large, every loading cycle leads to the accumulation of obvious damage in column CR302, and the lateral load capacity of column CR302 decreases after each loading cycle. All columns show the accumulation of obvious damage and reduction of load capacity at the displacement amplitude of 20-40 mm, but the load capacities of the three composite columns decrease more slowly than that of the RC column after the displacement amplitude surpasses 40 mm. Therefore, the CFST in the composite column can reduce the degree of damage to a column and make the column more stable under cyclic loads. Column CS302Ub showed perfect ductility throughout the loading test. With the displacement amplitude increasing, its load capacity remained very stable and decreased more slowly than did the other columns. This is because the concrete outside of CFST column was not subjected to axial load.

Lateral load capacities of columns CR302, CS302, CS302Ua and CS320Ub are respectively 85.5 kN, 129.4 kN, 115.2 kN and 102.7 kN. The lateral load capacity of column CR302 is the smallest. The lateral load capacity of column CS302 is the largest, and it is larger than that of column CR302 by 44%. The lateral load capacity of column CR302Ua is smaller than that of column CS302, but larger than that of column CR302. Thus, the CFST column in the composite column can markedly improve the lateral load capacity of the column, and the slip between concrete and tube reduces the lateral load capacity of the composite column. The lateral load capacity of column CS302Ub is 89.1% of that of column CS302Ua, which shows that the axial compression load in the RC column can lead to increment of lateral load capacity.

To compare the stiffness and ductility of the four columns, the envelopes of measured load-displacement relationships are depicted in Fig. 6. At the forehead loading stage, the stiffness and cracking load of column CS302Ub are smaller than those of other columns because the concrete outside of the CFST column was not subjected to axial load. The stiffness of columns CS302 and CS302Ua are nearly the same as that of column CR302 when the displacement is small, which shows that CFST with a small diameter has little influence on the initial flexural stiffness of composite column. However, the stiffness of columns CS302 and CS302Ua are greater than that of column CR302 when the displacement is large. From the comparison of columns CS302 and CS302Ua, it is can be seen that the influences of slip on the stiffness of a column become more obvious with increasing displacement.

3. Ductility

Ductility factor is usually used to evaluate the seismic response of reinforced concrete members (Légeron and Paultre, 2000; Paultre et al., 2001). The displacement ductility factor is defined as the ultimate displacement divided by the yield displacement. The ultimate displacement is defined as the displacement at 80% of the maximum lateral load in the descending portion of the lateral load-displacement relationship. The yield displacement is defined as the displacement obtained from the intersection point of the horizontal line at the maximum lateral load and the straight line from the origin passing through the point on the load-displacement plot at 75% of the maximum lateral load (Zahn et al., 1990). The definitions of maximum lateral load, ultimate displacement and yield displacement are shown in Fig. 7. The load-displacement relationship curve is the average of the envelope for the push-and-pull loading.

The ultimate displacements of the four columns, CR302, CS302, CS302Ua and CS320Ub, are respectively 59.9 mm, 71.2 mm, 73.7 mm and 87.1 mm. The yield displacements of the four columns are respectively 4.2 mm, 8.1 mm, 8.3 mm

Table 1. Comparison of responses.

Specimen	Maximum Force F_u(kN)	Yielding displacement u_y(mm)	Ultimate displacement u_u(mm)	Ultimate drift ratio u_u/L(%)	Ductility factor u_u/u_y
CR302	85.3	4.2	59.9	6.7	14.3
CS302	127.8	8.1	71.2	7.9	8.8
CS302Ua	112.9	8.3	73.7	8.2	8.9
CS302Ub	101.7	9.4	87.1	9.7	9.3

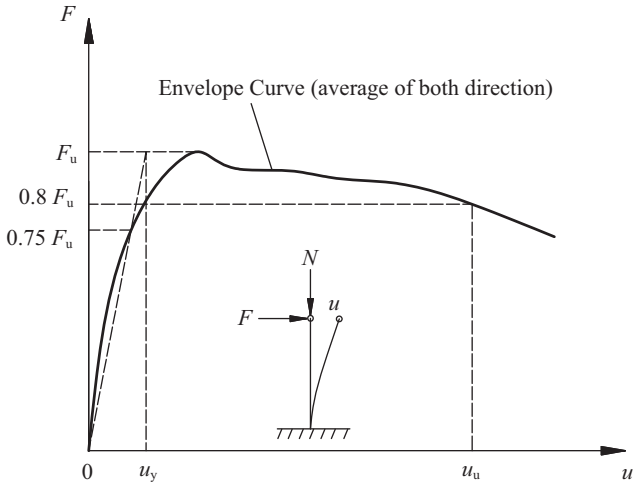

Fig. 7. Ideal curve definitions.

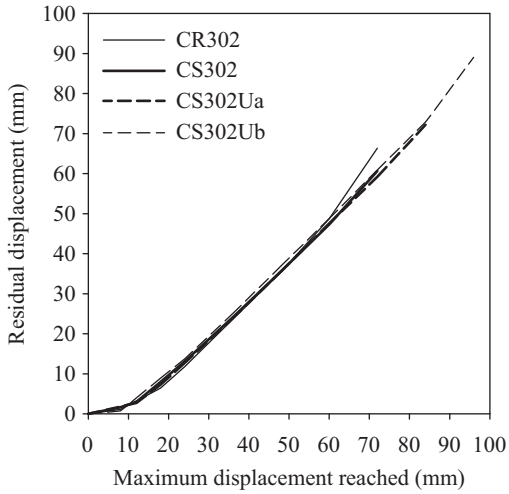

Fig. 8. Residual displacement comparison.

and 9.4 mm. Thus, the displacement ductility factors of the four columns are respectively 14.3, 8.8, 8.9 and 9.3. The ultimate drift ratios (defined as the ultimate displacement divided by the height of lateral loading point from the column footing) of the four columns are respectively 6.7%, 7.9%, 8.2% and 9.7%. The displacement ductility factor of column CR302 is the largest, and the displacement ductility factors of the other three columns are nearly the same. The ultimate drift ratio of column CS302Ub is the largest, so the deformation capacity of CS302Ub is the largest. The quantity comparison of the above items is listed in Table 1.

4. Residual Displacement

Residual displacement is a very important factor for determining whether a bridge undergoing a strong earthquake will be damaged or not. Large residual inclination of piers makes placing girders difficult and causes visual uneasiness even if repair is possible. After the Kobe earthquake, the piers with residual inclination larger than 1° were removed even if their visually judged damage was mild (Fujino et al., 2005). Therefore, reducing the residual displacement of piers is a very important part of improving the seismic performance of bridge columns.

Fig. 8 presents the relationships of the residual displacements of the four tested columns and the maximum displacements reached. When the displacement is smaller than 60 mm, the four curves are nearly overlapped, and the residual displacement of column CS302Ub is a bit larger. The relationships between residual displacement and displacement amplitude are nonlinear when displacement amplitude increases from 0 mm to 20 mm. The relationship curves become linear after displacement amplitude is larger than 30 mm. When the displacement amplitude is larger than the ultimate displacement of column CR302, the residual displacement of column CR302 increases very rapidly. Additionally, for every column, when the displacement amplitude does not reach its ultimate displacement, the residual displacements of three loading cycles at the same displacement amplitude change little, but the maximum lateral load decreases obviously after each loading cycle.

5. Energy Dissipation

The energy dissipation capacity is critically important for the seismic performance of a bridge column (Légeron and Paultre, 2000; Paultre et al., 2001). The dissipated energy can be determined by integrating the areas bounded by all the hysteretic loops throughout the entire loading test (Paultre et al., 2009). The energy dissipated in one loading cycle, as shown in Fig. 9, can be defined as follows:

$$E_i = \int_A^B F du$$

The total energy dissipated during the test until failure is

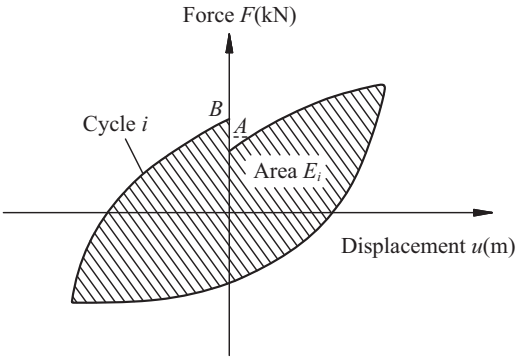

Fig. 9. Energy dissipation definition.

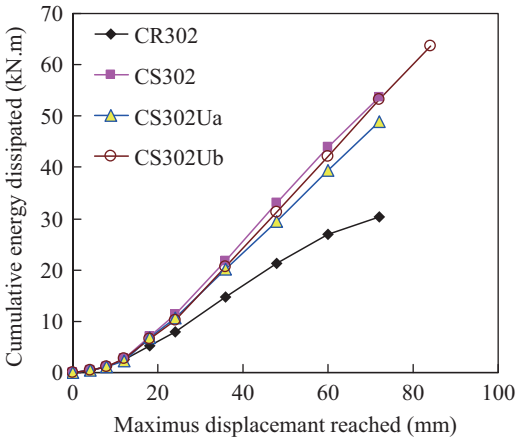

Fig. 10. Cumulative energy dissipation of specimens.

$$E_{hyst} = \sum_{i=1}^{n} E_i$$

where n is the number of cycles to failure.

Fig. 10 presents the cumulative energy dissipation-displacement amplitude relationships of the four tested columns. The curves of the three composite columns are very similar. When displacement is larger than 20 mm, the dissipated energy of the composite columns increases linearly with the maximum displacement reached, which shows that the composite columns have stable energy dissipation capacities. When displacement is small, the energy dissipation curve of the RC column is not obviously different from those of the composite columns. However, with increasing displacement, the difference between the RC column and the composite columns becomes larger and larger. The dissipated energy of the RC column increases nonlinearly with the maximum displacement reached, which shows that the energy dissipation capacity of RC column decreases with increasing displacement amplitude. It is concluded that a CFST column in a composite column can markedly improve the energy dissipation capacity of a bridge column, which is very beneficial for enhancing a bridge's resistance to strong earthquakes.

IV. CONCLUSIONS

Based on the experimental results in this paper, the following key conclusions can be reached:

1. A CFST column in a composite column can improve the flexural strength, shear strength and energy dissipation capacity of the column, and effectively avoid the shear failure and core crushing of the column. For the composite column with a diameter of 300 mm, a CFST column with a diameter of about 1/3 of that of the composite column diameter does not affect the concrete construction quality, and it is east to connect the CFST column with the footing. The lateral load capacity of the composite column is larger and more stable than that of the RC column. The energy dissipation capacity of the composite column is much larger than that of the RC column, especially when the displacement is large. This is very beneficial for enhancing a bridge's resistance to strong earthquakes.
2. The bond between the CFST column and the outside concrete has little effect on the energy dissipation capacity and residual displacement of the composite column. The slip between the CFST column and the outside concrete reduces the flexural strength of the composite column, but improves the ductility and deformation capacity of the composite column.
3. When axial compression load is only bone by the CFST column, the flexural strength of the composite column decreases dramatically, the ductility and deformation capacity of composite column is improved markedly, and the residual displacement and energy dissipation capacity of the composite column is affected very little.
4. Before the lateral tip displacement of a column reaches its ultimate displacement, the CFST column has little effect on the residual displacement. After the lateral displacement of column exceeds its ultimate displacement, the residual displacement of the RC column increases very quickly, but the residual displacement of the composite column increases stably with increasing lateral displacement.

ACKNOWLEDGMENTS

This study was funded by the National Natural Science Foundation of China (NSFC-51178080). The authors would like to acknowledge the Structure Engineering Laboratory of Dalian University of Technology for its support and constructive advice.

REFERENCES

Chen, W. F. and L. Duan (1999). Bridge Engineering Handbook. CRC press LLC, London.

Cusson, D. and P. Paultre (1994). High-strength concrete columns confined by rectangular ties. Journal of Structural Engineering 120(3), 783-804.

Fujino, Y., S. Hashimot and M. Abe (2005). Damage analysis of Hanshin expressway viaducts during 1995 Kobe Earthquake. I: residual inclination of reinforced concrete piers. Journal of Bridge Engineering 10(1),

45-53.

Hashimoto, S., Y. Fujino and M. Abe (2005). Damage analysis of Hanshin expressway viaducts during 1995 Kobe Earthquake. II: damage mode of single reinforced concrete Piers. Journal of Bridge Engineering 10(1), 54-60.

Hsu, Y. T. and C. C. Fu (2004). Seismic effect on highway bridges in Chi Chi Earthquake. Journal of Performance of Constructed Facilities 18(1), 869-879.

Kao, C. S. and C. H. Kou (2010). The influence of broken cables on the structural behavor of long-span cable-stayed bridges. Journal of Marine Science and Technology 18(3), 395-404,.

Kao, C. S., C. H. Kou, W. L. Qiu and J. L. Tsai (2010). Ultimate load-bearing capacity of self-anchored suspension bridges. Journal of Marine Science and Technology 20(1), 18-25.

Légeron, F. and P. Paultre (2000). Behavior of high-strength concrete columns under cyclic flexure and constant axial load. ACI Structure Journal 97(4), 591-601.

Pandey, G. R. and H. Mutsuyoshi (2005). Seismic performance of reinforced concrete piers with bond-controlled reinforcements. ACI Structure Journal 102(2), 295-304.

Paultre, P., F. Légeron and D. Mongeau (2001). Influence of concrete strength and yield strength of ties on the behavior of high-strength concrete columns. ACI Structure Journal 98(4), 490-501.

Paultre, P., R. Eid, H. I. Robles and N. Bouaanani (2009). Seismic performance of circular high-strength concrete columns. ACI Structure Journal 106(4), 395-404.

Razvi, S. R. and M. Saatcioglu (1994). Strength and deformability of confined high-strength concrete columns. ACI Structure Journal 91(6), 678-687.

Roeder, C. W. and D. E. Lehman (2009). Research on rapidly constructed CFT bridge piers suitable for seismic design. Lifeline Earthquake Engineering in a Multihazard Environment ASCE (TCLEE 2009), California, United States, 24-34.

Zahn, F. A., R. Park and M. J. N. Priestley (1990). Flexural strength and ductility of circular hollow reinforced concrete columns without confinement on inside face. ACI Structure Journal 87(2), 156-166.